

Radiative charged pion photoproduction and pion polarizabilities: An analysis within heavy baryon chiral perturbation theory

Chung-Wen Kao¹, Blaine E. Norum², and Kebin Wang²

¹*Department of Physics, North Carolina State University, Raleigh, NC27695-8202, USA and*

²*Department of Physics, University of Virginia, Charlottesville, VA22904-4714, USA*

(Dated: May 23, 2019)

We analyze the amplitude of radiative charged pion photoproduction in the framework of heavy baryon chiral perturbation theory and discuss the best kinematic conditions for the extraction of pion polarizabilities from the total cross section.

Electric (α) and magnetic (β) polarizabilities characterize the global deformation response of a composite system in static uniform external electric and magnetic fields. They provide precious information about the underlying dynamics of the composite system. As a result, a precise measurement of the pion polarizabilities is of great importance to understand the inner structure of the pion. Chiral symmetry allows one to predict the electromagnetic polarizabilities of charged pion in terms of the radiative decay $\pi^+ \rightarrow e^+ \nu_e \gamma$ [1],

$$\alpha_{\pi^\pm} = -\beta_{\pi^\pm} = \frac{e^2}{4\pi} \cdot \frac{2}{m_\pi (4\pi F_\pi)^2} \cdot \frac{l_6^r - l_5^r}{6} = \frac{\alpha_{em} h_A}{\sqrt{2} F_\pi m_\pi} = (2.64 \pm 0.09) \times 10^{-4} f m^3, \quad (1)$$

where $l_6^r - l_5^r$ is a linear combination of scale-independent parameters of the Gasser and Leutwyler Lagrangian [2]. $F_\pi = 93.1 MeV$ is the pion decay constant, $h_A = (0.0115 \pm 0.0004)/m_\pi$ [3] is the axial vector coupling constant. The next-to-leading-order result has been calculated at $\mathcal{O}(p^6)$ in Chiral Perturbation Theory(ChPT), and the correction to (1) is small: [4, 5]:

$$\begin{aligned} (\alpha + \beta)_{\pi^\pm} &= (0.3 \pm 0.1) \times 10^{-4} f m^3, \\ (\alpha - \beta)_{\pi^\pm} &= (4.4 \pm 1.0) \times 10^{-4} f m^3. \end{aligned} \quad (2)$$

Therefore the measurement of pion polarizabilities becomes an excellent test of chiral dynamics.

Compton scattering of real photons(RCS) is one of the simplest reactions to determine the polarizabilities. When expanded in the energy of final photon, the leading order term of the low-energy scattering amplitudes is specified by the Thomson limit in terms of the charge and the mass of the target. Genuine structure effects first appear at second order parametrized as polarizabilities.

$$T_{\gamma\pi \rightarrow \gamma\pi} = T_B + 8\pi m_\pi \omega \omega' [(\vec{\epsilon}_1 \cdot \vec{\epsilon}_2^*) \alpha_\pi + (\vec{k}' \times \vec{\epsilon}_2^*) \cdot (\vec{k} \times \vec{\epsilon}_1) \beta_\pi] + \dots \quad (3)$$

where $\vec{\epsilon}_1(\vec{\epsilon}_2)$, $\omega(\omega')$ and $\vec{k}(\vec{k}')$ are the polarization vector, energy and momentum of the initial (final) photon, respectively. T_B is the Born amplitude. Because pion targets are unavailable, RCS of pions was done by using indirect ways, such as high-energy pion-nucleus bremsstrahlung $\pi^- Z \rightarrow \pi^- Z \gamma$ [6] or radiative pion photoproduction off the proton $\gamma p \rightarrow \gamma \pi^+ n$ [7] and the cross channel two-photon reaction $\gamma \gamma \rightarrow \pi \pi$ [8, 9]. Recently the new radiative charged pion photoproduction experiment at Mainz Microtron MAMI [10] reported their result which is far away from the prediction of ChPT,

$$(\alpha - \beta)_{\pi^\pm} = (11.6 \pm 1.5_{stat} \pm 3.0_{syst} \pm 0.5_{model}) \times 10^{-4} f m^3. \quad (4)$$

In this letter, we investigate the relation between the charged pion polarizabilities and the radiative charged pion photoproduction in the framework of heavy baryon chiral perturbation theory(HBChPT). (see [11] for a review of HBChPT.) So far, the extractions of charged pion polarizabilities α_{π^\pm} and β_{π^\pm} from radiative charged pion photoproduction have relied on two different ways. The method of extrapolation [12, 13] is similar to the one suggested by Chew and Low [14] in the late fifties. This method has been successfully employed to determine the pion-nucleon coupling constant through $\gamma p \rightarrow \pi^+ p$. It is also used in the determination of $\pi\pi \rightarrow \pi\pi$ scattering from $\pi N \rightarrow \pi\pi N$ reaction. However, in order to do extrapolation, one has to obtain the experimental data with small error over a sufficiently wide region of t , particularly when very close to $t=0$. The authors of [10] also point out that the pion pole diagram alone is not gauge invariant, and one has take into account all the pion and nucleon pole amplitudes. Therefore the applicability of extrapolation method is in doubt.

The second way is to use models to calculate the cross section of the reaction $\gamma p \rightarrow \gamma \pi^+ n$. For example, in [10] they

adopt two different models. The first one includes all the pion and nucleon pole diagrams by using pseudoscalar pion-nucleon coupling. The second one is to include the nucleon and pion pole diagrams (without the anomalous magnetic moments of the nucleons and the contributions) from the resonances $\Delta(1232)$, $P_{11}(1440)$, $D_{13}(1520)$, $S_{11}(1535)$. Then they determine the value of $(\alpha - \beta)_{\pi^\pm}$ from comparing the experimental data with predictions of these two models.

HBChPT provides a third way. The cross section of the reaction $\gamma p \rightarrow \pi^+ \gamma n$ can be calculated within HBChPT and expressed as a function of α_{π^\pm} and β_{π^\pm} . This approach is model-independent. It is also conceptually more consistent because the effects of chiral loops on pions and nucleons are treated equally. The result of the complete calculation of the radiative pion photoproduction in HBChPT at one-loop level will be reported elsewhere [15]. In this letter we will focus on the best kinematics and polarization conditions for the extraction of charged pion polarizabilities from the cross section of radiative charged pion photoproduction.

In the following we adopt the conventions:

$$\gamma(\epsilon_1, k) + p(P_1) \rightarrow \gamma(\epsilon_2, q) + \pi^+(r) + n(P_2). \quad (5)$$

$\epsilon_1(\epsilon_2)$ and $k(q)$ are the polarization vector and momentum of incoming(outgoing) photon, respectively. As an effective field theory, the HBChPT gives the gauge invariant amplitude order by order. Therefore we are free to choose the most convenient gauge. We choose this gauge: $\epsilon_1 \cdot v = \epsilon_2 \cdot v = 0$. Here v is the velocity of the nucleon and is taken as $v_\mu = (1, \vec{0})$. The gauge condition becomes Coulomb gauge: $\epsilon_1^0 = \epsilon_2^0 = 0$. Such a choice of gauge simplifies the computation greatly because in this gauge the leading order γNN vertex vanishes. Also $\vec{\epsilon}_1 \cdot \vec{k} = \vec{\epsilon}_2 \cdot \vec{q} = 0$ because both of the incoming and the outgoing photons are real. HBChPT allows one to choose the most convenient frame. In general, $k = (\omega_k, \vec{k})$, $q = (\omega_q, \vec{q})$, $r = (\omega_r, \vec{r})$. $P_1 = (\sqrt{M_N^2 + |\vec{p}_1|^2}, \vec{p}_1)$, $P_2 = (\sqrt{M_N^2 + |\vec{p}_2|^2}, \vec{p}_2)$. By energy conservation, one gets the relation for the small momentum transfer,

$$\omega_k - \omega_q - \omega_r = \sqrt{M_N^2 + |\vec{p}_2|^2} - \sqrt{M_N^2 + |\vec{p}_1|^2} \sim \mathcal{O}\left(\frac{1}{M_N}\right). \quad (6)$$

The most convenient frame here is the c.m. frame of the final $\gamma - \pi$ system. In this frame, one has

$$\begin{aligned} S_1 &\equiv (r + q)^2 = (\omega_q + \omega_r)^2, \quad t \equiv (P_1 - P_2)^2 = (r - k + q)^2, \quad \cos\theta \equiv \hat{k} \cdot \hat{q}, \\ \omega_q &= \frac{S_1 - m_\pi^2}{2\sqrt{S_1}}, \quad \omega_k = \frac{S_1 - t}{2\sqrt{S_1}}, \quad \omega_r = \frac{S_1 + m_\pi^2}{2\sqrt{S_1}}, \\ u &\equiv (r - k)^2 = \frac{1}{2} \left(m_\pi^2 + t - S_1 + \frac{tm_\pi^2}{S_1} \right) + \frac{\cos\theta}{2} \left(m_\pi^2 - S_1 + t - \frac{tm_\pi^2}{S_1} \right). \end{aligned} \quad (7)$$

In this letter we call the plane spanned by \vec{k} and \vec{r} “scattering plane”.

One has to decide to which order the amplitudes need to be computed in HBChPT. Note that HBChPT essentially is a double expansion, i.e., the combination of the chiral expansion and heavy baryon expansion. The amplitudes can be expressed as :

$$\mathcal{A} = \sum_{n=0, m=0}^{\infty} \frac{\mathcal{B}_{m,n}}{(M_N)^n (4\pi F_\pi)^{2m}} = \sum_{l=2m+n}^{\infty} \mathcal{A}^{(l)}. \quad (8)$$

The prediction of the pion polarizabilities (1) is the result of the calculation of pion RCS at one loop level, so α_{π^\pm} and β_{π^\pm} emerges at $\mathcal{A}^{(2)}(m=1, n=0)$. Therefore one has to calculate up to the next-next-leading order in HBChPT in addition to $\mathcal{A}^{(0)}(n=0, m=0)$ and $\mathcal{A}^{(1)}(n=1, m=0)$. The leading-order(LO) amplitude \mathcal{A}_{LO} is $\mathcal{A}^{(0)}(n=0, m=0)$, and the next-leading-order(NLO) amplitude \mathcal{A}_{NLO} is $\mathcal{A}^{(1)}(n=1, m=0)$. The square of the amplitude will be expressed as

$$\begin{aligned} \mathcal{A} &= \mathcal{A}_{LO} + \mathcal{A}_{NLO} + \mathcal{A}_{NNLO} + \dots, \quad |\mathcal{A}|^2 = |\mathcal{A}_{LO}|^2 \\ &\quad + 2Re(\mathcal{A}_{LO}\mathcal{A}_{NLO}^*) \\ &\quad + 2Re(\mathcal{A}_{LO}\mathcal{A}_{NNLO}^*) + |\mathcal{A}_{NLO}|^2 + \dots \end{aligned} \quad (9)$$

The LO and NLO diagrams are given in the Fig(1) and Fig(2) respectively. The LO amplitudes of the radiative pion photoproduction are given in the following:

$$\mathcal{A}_{1A} = \frac{-e^2 g_A}{F_\pi} [\tau_c - \tau_3 \delta_{c3}] \frac{(\vec{\epsilon}_1 \cdot \vec{\epsilon}_2^*)(\vec{\sigma} \cdot (\vec{r} - \vec{k} + \vec{q}))}{t - m_\pi^2},$$

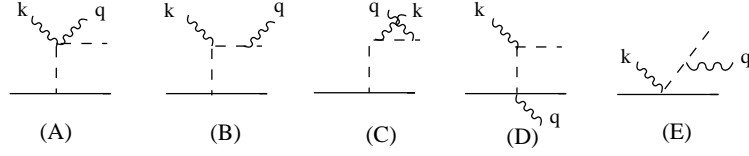


FIG. 1: The LO diagrams of radiative pion electroproduction in the Coulomb gauge.

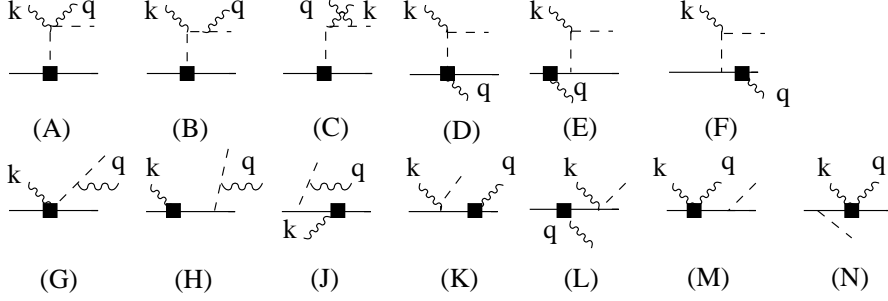


FIG. 2: The NLO diagrams of radiative pion electroproduction in Coulomb gauge. The squares represent the LO vertices from $\mathcal{L}_{\pi N}^{(2)}$ or the NLO vertices of $\mathcal{L}_{\pi N}^{(1)}$. Here LO (NLO) mean the leading(next-to-leading) terms in the heavy baryon expansion.

$$\begin{aligned}
\mathcal{A}_{1B} &= \frac{-2e^2 g_A}{F_\pi} [\tau_c - \tau_3 \delta_{c3}] \frac{(\vec{\epsilon}_2^* \cdot \vec{r})(\vec{\epsilon}_1 \cdot (\vec{r} + \vec{q}))(\vec{\sigma} \cdot (\vec{r} - \vec{k} + \vec{q}))}{[S_1 - m_\pi^2][t - m_\pi^2]}, \\
\mathcal{A}_{1C} &= \frac{-2e^2 g_A}{F_\pi} [\tau_c - \tau_3 \delta_{c3}] \frac{(\vec{\epsilon}_1 \cdot \vec{r})(\vec{\epsilon}_2^* \cdot (\vec{r} - \vec{k}))(\vec{\sigma} \cdot (\vec{r} - \vec{k} + \vec{q}))}{[u - m_\pi^2][t - m_\pi^2]}, \\
\mathcal{A}_{1D} &= \frac{-e^2 g_A}{F_\pi} [\tau_c - \tau_3 \delta_{c3}] \frac{(\vec{\epsilon}_1 \cdot \vec{r})(\vec{\sigma} \cdot \vec{\epsilon}_2^*)}{u - m_\pi^2}, \\
\mathcal{A}_{1E} &= \frac{-e^2 g_A}{F_\pi} [\tau_c - \tau_3 \delta_{c3}] \frac{(\vec{\epsilon}_2^* \cdot \vec{r})(\vec{\sigma} \cdot \vec{\epsilon}_1)}{S_1 - m_\pi^2}.
\end{aligned} \tag{10}$$

Here c is isospin index of the outgoing pion and $*$ represents complex conjugate. There are several remarks about the LO amplitudes. First of all, they are all nucleon spin-flip. Secondly, the diagrams such as (1-B), (1-C), (1-D), and (1-E) are not present in the process of $\pi N \rightarrow \pi\pi N$ because there is no 3π vertex at the leading order. This point is important because it explains the essential difference between $\pi N \rightarrow \pi\pi N$ and $\gamma p \rightarrow \gamma\pi^+ n$. We will return to this point when we discuss the extrapolation. Furthermore, diagrams (1-B) and (1-E) both vanish in the c.m. frame of the final $\gamma - \pi$ system because $\vec{\epsilon}_2^* \cdot \vec{r} = \vec{\epsilon}_2^* \cdot \vec{q} = 0$. Also, diagrams (1-C) and (1-D) will vanish if the polarization vector of the incoming photon is perpendicular to the scattering plane spanned by \vec{k} and \vec{r} .

The NLO amplitudes are given as following:

$$\begin{aligned}
\mathcal{A}_{2A} &= \frac{e^2 g_A}{2M_N F_\pi} [\tau_c - \tau_3 \delta_{c3}] \frac{(\vec{\epsilon}_1 \cdot \vec{\epsilon}_2^*)(\vec{\sigma} \cdot (\vec{p}_1 + \vec{p}_2))}{t - m_\pi^2} \cdot (\omega_q + \omega_r - \omega_k), \\
\mathcal{A}_{2B} &= \frac{e^2 g_A}{M_N F_\pi} [\tau_c - \tau_3 \delta_{c3}] \frac{(\vec{\epsilon}_2^* \cdot \vec{r})(\vec{\epsilon}_1 \cdot (\vec{r} + \vec{q}))(\vec{\sigma} \cdot (\vec{p}_1 + \vec{p}_2))}{[S_1 - m_\pi^2][t - m_\pi^2]} \cdot (\omega_q + \omega_r - \omega_k), \\
\mathcal{A}_{2C} &= \frac{e^2 g_A}{M_N F_\pi} [\tau_c - \tau_3 \delta_{c3}] \frac{(\vec{\epsilon}_1 \cdot \vec{r})(\vec{\epsilon}_2^* \cdot (\vec{r} - \vec{k}))(\vec{\sigma} \cdot (\vec{p}_1 + \vec{p}_2))}{[u - m_\pi^2][t - m_\pi^2]} \cdot (\omega_q + \omega_r - \omega_k), \\
\mathcal{A}_{2D} &= \frac{e^2 g_A}{4M_N F_\pi} [\tau_c, \tau_3] \frac{(\vec{\epsilon}_1 \cdot \vec{r})(\vec{\sigma} \cdot \vec{\epsilon}_2^*)}{u - m_\pi^2} \cdot (\omega_r - \omega_k), \\
\mathcal{A}_{2E} &= \frac{-e^2 g_A}{2M_N F_\pi} [\tau_c \tau_3 - \delta_{c3}] [1 + \tau_3] \frac{(\vec{\epsilon}_1 \cdot \vec{r})(\vec{\sigma} \cdot (\vec{r} - \vec{k}))(\vec{\epsilon}_2^* \cdot \vec{p}_1)}{u - m_\pi^2} \cdot \frac{1}{\omega_q},
\end{aligned}$$

$$\begin{aligned}
& - \frac{e^2 g_A}{8M_N F_\pi} [\tau_c \tau_3 - \delta_{c3}] \tilde{\mu} \frac{(\vec{\epsilon}_1 \cdot \vec{r}) (\vec{\sigma} \cdot (\vec{r} - \vec{k})) (\vec{\sigma} \cdot \vec{\epsilon}_2^*, \vec{\sigma} \cdot \vec{q})}{u - m_\pi^2} \cdot \frac{1}{\omega_q}, \\
\mathcal{A}_{2F} &= \frac{e^2 g_A}{2M_N F_\pi} [1 + \tau_3] [\tau_c \tau_3 - \delta_{c3}] \frac{(\vec{\epsilon}_1 \cdot \vec{r}) (\vec{\sigma} \cdot (\vec{r} - \vec{k})) (\vec{\epsilon}_2^* \cdot \vec{p}_2)}{u - m_\pi^2} \cdot \frac{1}{\omega_q}, \\
& + \frac{e^2 g_A}{8M_N F_\pi} \tilde{\mu} [\tau_c \tau_3 - \delta_{c3}] \frac{(\vec{\epsilon}_1 \cdot \vec{r}) (\vec{\sigma} \cdot \vec{\epsilon}_2^*, \vec{\sigma} \cdot \vec{q}) (\vec{\sigma} \cdot (\vec{r} - \vec{k}))}{u - m_\pi^2} \cdot \frac{1}{\omega_q}, \\
\mathcal{A}_{2G} &= \frac{e^2 g_A}{4M_N F_\pi} [\tau_c, \tau_3] \frac{(\vec{\epsilon}_2^* \cdot \vec{r}) (\vec{\sigma} \cdot \vec{\epsilon}_1)}{S_1 - m_\pi^2} \cdot (\omega_r + \omega_q), \\
\mathcal{A}_{2H} &= \frac{e^2 g_A}{2M_N F_\pi} [\tau_c \tau_3 - \delta_{c3}] [1 + \tau_3] \frac{(\vec{\epsilon}_2^* \cdot \vec{r}) (\vec{\sigma} \cdot (\vec{r} + \vec{q})) (\vec{\epsilon}_1 \cdot \vec{p}_1)}{S_1 - m_\pi^2} \cdot \frac{1}{\omega_k}, \\
& + \frac{e^2 g_A}{8M_N F_\pi} [\tau_c \tau_3 - \delta_{c3}] \tilde{\mu} \frac{(\vec{\epsilon}_2^* \cdot \vec{r}) (\vec{\sigma} \cdot (\vec{r} + \vec{q})) (\vec{\sigma} \cdot \vec{\epsilon}_1, \vec{\sigma} \cdot \vec{k})}{S_1 - m_\pi^2} \cdot \frac{1}{\omega_k}, \\
\mathcal{A}_{2J} &= \frac{-e^2 g_A}{2M_N F_\pi} [1 + \tau_3] [\tau_c \tau_3 - \delta_{c3}] \frac{(\vec{\epsilon}_2^* \cdot \vec{r}) (\vec{\sigma} \cdot (\vec{r} + \vec{q})) (\vec{\epsilon}_1 \cdot \vec{p}_2)}{S_1 - m_\pi^2} \cdot \frac{1}{\omega_k}, \\
& - \frac{e^2 g_A}{8M_N F_\pi} \tilde{\mu} [\tau_c \tau_3 - \delta_{c3}] \frac{(\vec{\epsilon}_2^* \cdot \vec{r}) (\vec{\sigma} \cdot \vec{\epsilon}_1, \vec{\sigma} \cdot \vec{k}) (\vec{\sigma} \cdot (\vec{r} + \vec{q}))}{S_1 - m_\pi^2} \cdot \frac{1}{\omega_q}, \\
\mathcal{A}_{2K} &= \frac{-e^2 g_A}{4M_N F_\pi} [1 + \tau_3] [\tau_c \tau_3 - \delta_{c3}] \frac{(\vec{\epsilon}_2^* \cdot \vec{p}_2) (\vec{\sigma} \cdot \vec{\epsilon}_1)}{\omega_k - \omega_r} \\
& - \frac{e^2 g_A}{16M_N F_\pi} \tilde{\mu} [\tau_c \tau_3 - \delta_{c3}] [1 + \tau_3] \frac{[\vec{\sigma} \cdot \vec{\epsilon}_2^*, \vec{\sigma} \cdot \vec{q}] (\vec{\sigma} \cdot \vec{\epsilon}_1)}{\omega_k - \omega_r}, \\
\mathcal{A}_{2L} &= \frac{e^2 g_A}{4M_N F_\pi} [\tau_c \tau_3 - \delta_{c3}] [1 + \tau_3] \frac{(\vec{\epsilon}_1 \cdot \vec{p}_1) (\vec{\sigma} \cdot \vec{\epsilon}_2^*)}{\omega_q + \omega_r} \\
& + \frac{e^2 g_A}{16M_N F_\pi} [\tau_c \tau_3 - \delta_{c3}] \tilde{\mu} \frac{[\vec{\sigma} \cdot \vec{\epsilon}_1, \vec{\sigma} \cdot \vec{k}] (\vec{\sigma} \cdot \vec{\epsilon}_2^*)}{\omega_q + \omega_r}, \\
\mathcal{A}_{2M} &= \frac{-e^2 g_A}{4M_N F_\pi} \tau_c (1 + \tau_3) \frac{(\vec{\sigma} \cdot \vec{r}) (\vec{\epsilon}_1 \cdot \vec{\epsilon}_2^*)}{\omega_r}, \\
\mathcal{A}_{2N} &= \frac{e^2 g_A}{4M_N F_\pi} (1 + \tau_3) \tau_c \frac{(\vec{\sigma} \cdot \vec{r}) (\vec{\epsilon}_1 \cdot \vec{\epsilon}_2^*)}{\omega_r}, \tag{11}
\end{aligned}$$

where $\tilde{\mu} = (1 + \kappa_s) + \tau_3(1 + \kappa_v)$. $\kappa_v(\kappa_s) = 3.76(-0.120)$ are the isovector (isoscalar) anomalous magnetic moment of the nucleon. The first three diagrams (2-A),(2-B) and (2-C) do not contribute to the NLO amplitudes because $\omega_k - \omega_q - \omega_r \sim \mathcal{O}\left(\frac{1}{M_N}\right)$. The diagrams (2-G) and (2-H) and (2-J) all vanish in the c.m. frame of the final $\gamma - \pi$ system because $\vec{\epsilon}_2^* \cdot \vec{r} = \vec{\epsilon}_2^* \cdot \vec{q} = 0$. The diagrams (2-D), (2-E) and (2-F) will vanish if the polarization vector of the incoming photon is perpendicular to the scattering plane.

The NNLO amplitude include $\mathcal{A}^{(2)}(n = 2, m = 1)$ and $\mathcal{A}^{(2)}(n = 0, m = 1)$. The diagrams which contribute to $\mathcal{A}^{(2)}(n = 2, m = 1)$ are given by Fig(3). The diagrams which contribute to $\mathcal{A}_{(2)}(n = 0, m = 1)$ are given by (Fig(4)).

The ‘‘bubbles’’ from \mathcal{M}_A to \mathcal{M}_H are the sums of one-particle-irreducible diagrams of some sub-processes. (see Fig(5)). All can be calculated by HBChPT and actually most of them have been calculated before. Z_π and Z_N is the wavefunction renormalization factor of pion and nucleon, respectively. $\mathcal{M}_A(\gamma + \pi^+ \rightarrow \gamma + \pi^+)$ stands for the Compton scattering of the virtue incoming pion. If the incoming photon is also virtual, then this sub-diagram also carry the information of so-called generalized polarizability as studied in [16, 17]. $\mathcal{M}_B(\pi \rightarrow \pi)$ represents the renormalization of the pion mass. $\mathcal{M}_C(p \rightarrow \pi^+ + n)$ is the renormalization of the axial form factor of the nucleon. $\mathcal{M}_D(\pi^- + p \rightarrow \gamma + n)$ is the radiative virtual charged pion capture[18]. $\mathcal{M}_E(\pi^+ \rightarrow \gamma + \pi^+)$ is the pion electromagnetic form factor. $\mathcal{M}_F(\gamma + N \rightarrow \gamma + N)$ represents the Compton scattering of off-shell nucleon (either incoming or outgoing) [19]. $\mathcal{M}_G(N \rightarrow \gamma + N)$ stands for the nucleon electromagnetic form factor. The only sub-diagram that has never been calculated in HBChPT is $\mathcal{M}_H(\gamma + p \rightarrow \pi^+ + \gamma + n)$. \mathcal{M}_H are quite lengthy so we put them in the appendix.

Besides, there is one exceptional class of diagrams which are consisted of Wess-Zumino-Witten anomalous [20] term $\pi^0 \rightarrow 2\gamma$ (see Fig(6)). The WZW term is the consequence of the chiral anomaly of QCD [21]. These diagrams contribute to the NNLO amplitudes:

$$\mathcal{A}_A^{WZW} = i \frac{e^2}{8(4\pi F_\pi)^2 F_\pi} [\tau_3, \tau_c] \epsilon_{\mu\nu\alpha\beta} k^\mu \epsilon_1^\nu q^\alpha \epsilon_2^{*\beta} \frac{1}{(q - k)^2 - m_\pi^2} \cdot (\omega_k - \omega_q + \omega_r),$$

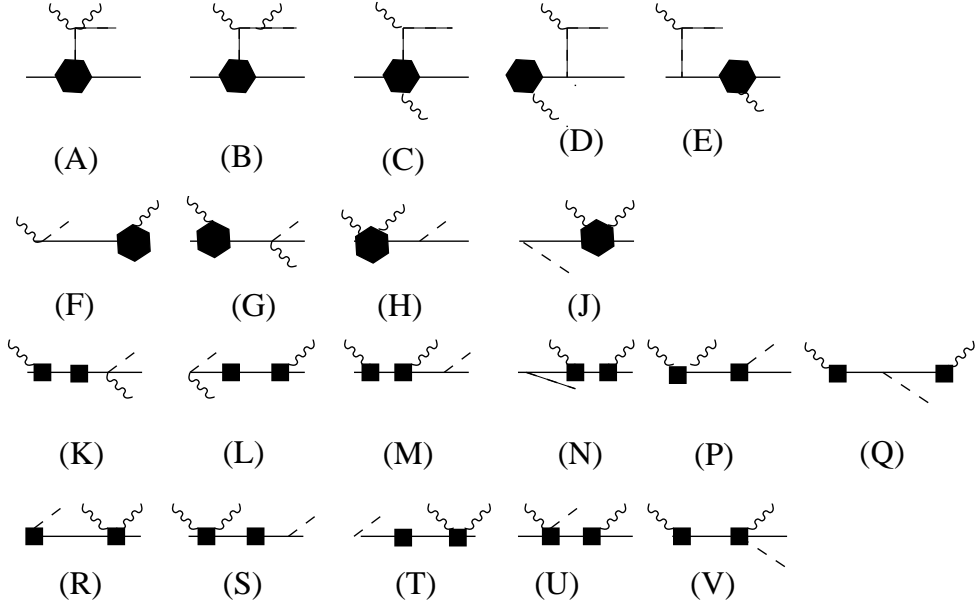


FIG. 3: The NNLO diagrams of radiative pion electroproduction in Coulomb gauge. The squares represent the LO vertices from $\mathcal{L}_{\pi N}^{(2)}$ or NLO expansion of $\mathcal{L}_{\pi N}^{(1)}$. The sextagon represent the NLO vertices from $\mathcal{L}_{\pi N}^{(2)}$ or NNLO vertices from $\mathcal{L}_{\pi N}^{(1)}$. Here NLO(NNLO) means the next-to-leading (next-next-leading) terms in the heavy baryon expansion only.

$$\begin{aligned}
\mathcal{A}_B^{WZW} &= -\frac{e^2 g_A^2}{4(4\pi F_\pi)^2 F_\pi} \tau_3 \tau_c \epsilon_{\mu\nu\alpha\beta} k^\mu \epsilon_1^\nu q^\alpha \epsilon_2^{*\beta} \frac{(\vec{\sigma} \cdot (\vec{q} - \vec{k}))(\vec{\sigma} \cdot \vec{r})}{(q-k)^2 - m_\pi^2} \frac{1}{\omega_r}, \\
\mathcal{A}_C^{WZW} &= \frac{e^2 g_A^2}{4(4\pi F_\pi)^2 F_\pi} \tau_c \tau_3 \epsilon_{\mu\nu\alpha\beta} k^\mu \epsilon_1^\nu q^\alpha \epsilon_2^{*\beta} \frac{(\vec{\sigma} \cdot \vec{r})(\vec{\sigma} \cdot (\vec{q} - \vec{k}))}{(q-k)^2 - m_\pi^2} \frac{1}{\omega_r}, \\
\mathcal{A}_B^{WZW} + \mathcal{A}_C^{WZW} &= \frac{e^2 g_A^2}{4(4\pi F_\pi)^2 F_\pi} \epsilon_{\mu\nu\alpha\beta} k^\mu \epsilon_1^\nu q^\alpha \epsilon_2^{*\beta} \\
&\quad \cdot \frac{1}{\omega_r} \left\{ [\tau_c, \tau_3] \frac{\vec{r} \cdot (\vec{q} - \vec{k})}{(q-k)^2 - m_\pi^2} - 2\delta_{c3} \frac{i\vec{\sigma} \cdot (\vec{q} - \vec{k}) \times \vec{r}}{(q-k)^2 - m_\pi^2} \right\}. \tag{12}
\end{aligned}$$

The incoming proton is unpolarized so total amplitude of $\gamma + p \rightarrow \gamma + \pi^+ + n$ is non-spinflip. Since \mathcal{A}_{LO} is spin-flip, only the spin-flip amplitude of \mathcal{A}_{NNLO} will contribute. As one can see from (12) the total amplitude of the leading order of WZW type diagrams is non-spinflip. Therefore, the WZW type diagrams do not contribute to the cross section in (9).

Now we can discuss the method of extrapolation in [7, 13]. The idea of extrapolation is to extrapolate the experimental data of $\gamma + p \rightarrow \gamma + n + \pi^+$ at small $t = t_{min} < 0$, to the pion pole $t = m_\pi^2$. By this way one can obtain the elastic $\gamma\pi^+$ scattering cross section. When t is small the pion-pole diagrams is supposed to be dominant. Therefore, in [7] only the diagrams with a pole at $t = m_\pi^2$, such as diagrams from (4-1) to (4-16), are considered,

$$\mathcal{A} \simeq \mathcal{M}(p \rightarrow \pi^+ + n) \cdot \frac{i}{t - m_\pi^2} \cdot \mathcal{M}(\pi^+ + \gamma \rightarrow \pi^+ + \gamma), \tag{13}$$

then one has

$$\frac{d^3 \sigma_{\gamma N \rightarrow \gamma \pi N}}{dt dS_1 d\Omega} \propto |\mathcal{A}|^2 \simeq \frac{|\mathcal{M}(\pi^+ + \gamma \rightarrow \pi^+ + \gamma)|^2 \cdot |\mathcal{M}(p \rightarrow \pi^+ + n)|^2}{(t - m_\pi^2)^2}. \tag{14}$$

Consequently, one has Chew-Low relation

$$\frac{d^3 \sigma_{\gamma N \rightarrow \gamma \pi N}}{dt dS_1 d\Omega} = \frac{g^2}{4\pi} \frac{S_1 - m_\pi^2}{8\pi M_p^2 E_\gamma^2} \frac{(-t)}{(t - m_\pi^2)^2} [G_A(t)]^2 \left(\frac{d\sigma}{d\Omega} \right)_{\gamma\pi \rightarrow \gamma\pi} + \dots, \tag{15}$$

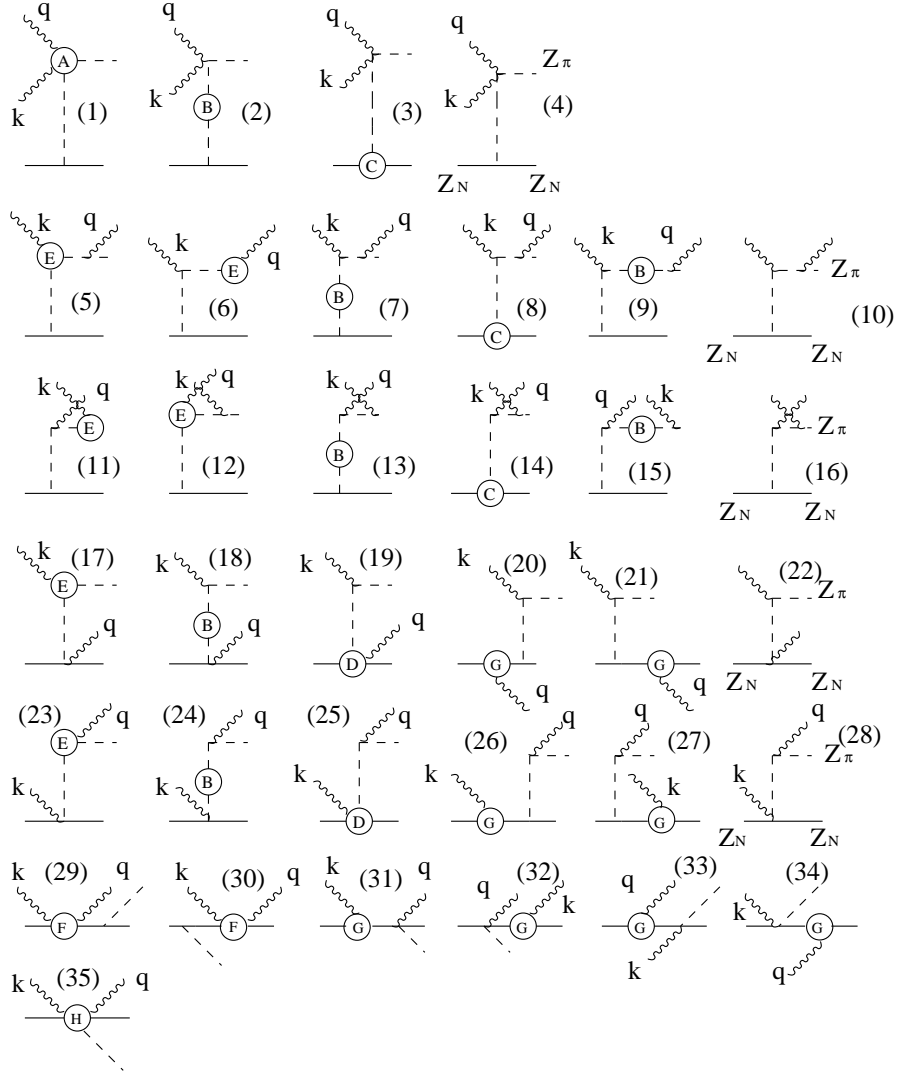


FIG. 4: The NNLO diagrams of radiative pion electroproduction in Coulomb gauge. The bubble of A to H represent the sub-diagrams.

where $\frac{g^2}{4\pi} = 14.7$ is the pion-nucleon coupling constant and the ellipsis represents the contribution of other diagrams. To remove the pole at $t = m_\pi^2$, one defines the following quantity,

$$F(t) \equiv (t - m_\pi^2)^2 \cdot \frac{d^3\sigma_{\gamma N \rightarrow \gamma\pi N}}{dt dS_1 d\Omega} (2E_\gamma M_p)^2 \rightarrow \frac{-g^2}{8\pi^2} (S_1 - m_\pi^2) t \cdot [G_A(t)]^2 \left(\frac{d\sigma}{d\Omega} \right)_{\gamma\pi \rightarrow \gamma\pi} + (t - m_\pi^2)^2 \cdot F_R(t, S_1, \theta), \quad (16)$$

here F_R stands for the contribution of all other diagrams without the $1/(t - m_\pi)$ pole and it is skipped because it is supposed to be small when $t = t_{min}$ is small. The final step is to use experimental data of $F(t)$ at small $t_{min} \leq 0$ to extrapolate to the pion pole.

$$\lim_{t \rightarrow m_\pi^2} F(t) \rightarrow \frac{-g^2}{8\pi^2} (S_1 - m_\pi^2) m_\pi^2 \cdot [G_A(t = m_\pi^2)]^2 \times \left(\frac{d\sigma}{d\Omega} \right)_{\gamma\pi \rightarrow \gamma\pi}^{elastic}. \quad (17)$$

Such a procedure is used to extract $\pi\pi$ scattering from $\pi N \rightarrow \pi\pi N$. However, here we can see that the extrapolation in the radiative pion photoproduction will be more complicated than in $\pi N \rightarrow \pi\pi N$. Even at the leading order, there is a diagrams (1-D) which does not have poles at $t = m_\pi^2$ but at $u = m_\pi^2$. By the power counting we can see

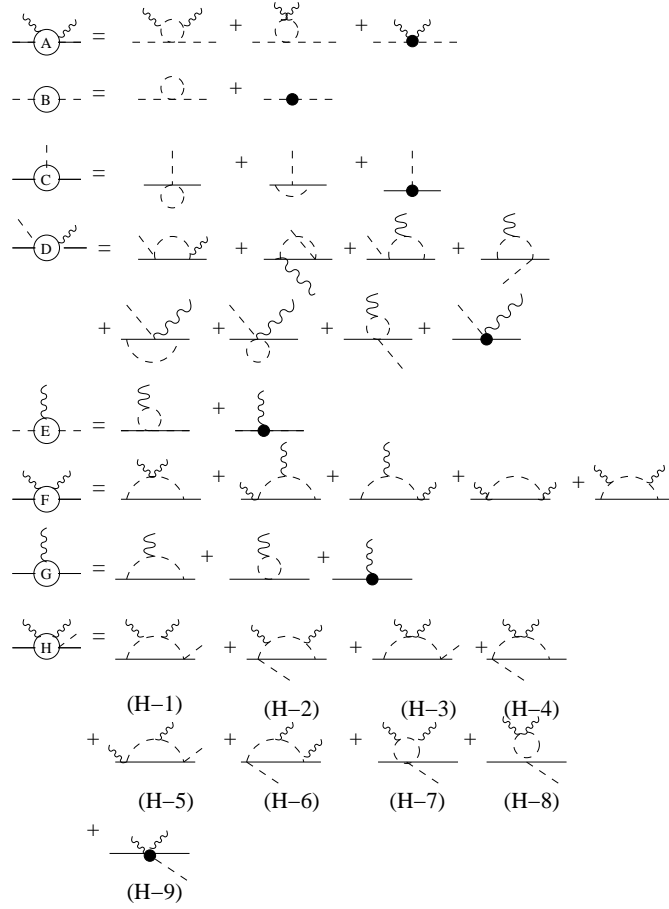


FIG. 5: The sub-diagrams from A to H. The full square represents the vertex from $\mathcal{L}_{\pi N}^{(2)}$, and the full circle represents the vertex from the $\mathcal{L}_{\pi N}^{(3)}$ or $\mathcal{L}_{\pi\pi}^{(4)}$.

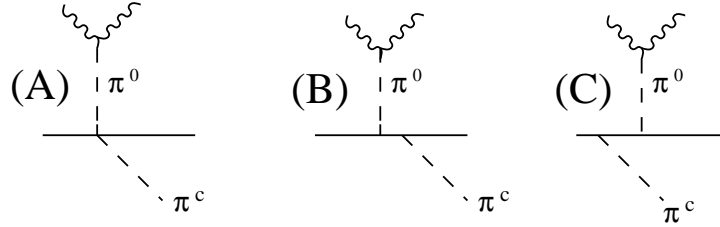


FIG. 6: The diagrams of the radiative pion electroproduction in the Coulomb gauge with the WZW vertex.

such a diagram cannot be neglected even at small t . Moreover, the value of $|\frac{1}{u-m_\pi^2}|$ becomes large when the angle θ moves toward the backward direction. Therefore the result of extrapolation will be away from the correct values of $(\frac{d\sigma}{d\Omega})_{\gamma\pi\rightarrow\gamma\pi}^{elastic}$, particularly at backward direction. The diagram (1-D) must be included because it is required by gauge invariance. There is only one exception. It can be shown that if the incoming photon is polarized along the direction perpendicular to the scattering plane spanned by \vec{k} and \vec{r} , all diagrams with $1/(u-m_\pi^2)$ vanish. So maybe the procedure of extrapolation is applicable in such as a polarization condition if other diagrams such as nucleon pole diagrams are suppressed at small t region. But it needs the complete calculation [15] to see whether it is a good

approximation.

In addition to the extrapolation, one may try to extract α_{π^\pm} and β_{π^\pm} from the total cross section of the radiative pion photoproduction. There is no unknown parameters in the LO and NLO amplitudes. According to (9), The cross section depends on the pion polarizabilities through the interference term of \mathcal{A}_{LO} and \mathcal{A}_{3-1} . The main uncertainty of this approach comes from the contributions of the other unknown parameters which are the coefficients of the counterterms in the chiral Lagrangian. They are so-called low energy constants (LECs).

The chiral Lagrangian is expanded in the following way,

$$\mathcal{L}_{eff} = \mathcal{L}_{\pi\pi}^{(2)} + \mathcal{L}_{\pi\pi}^{(4)} + \mathcal{L}_{\pi N}^{(1)} + \mathcal{L}_{\pi N}^{(2)} + \mathcal{L}_{\pi N}^{(3)} + \dots, \quad (18)$$

The pion polarizabilities α_{π^\pm} and β_{π^\pm} are determined by the LECs of $\mathcal{L}_{\pi\pi}^{(4)}$. There are 7 LECs in $\mathcal{L}_{\pi N}^{(2)}$ but only two are involved in our calculation and they are just the isovector and isoscalar anomalous magnetic moment of the nucleon, κ_s and κ_v . \mathcal{M}_B contains two LECs in $\mathcal{L}_{\pi\pi}^{(4)}$ but they are absorbed into the renormalized pion mass. Similarly \mathcal{M}_C also contains two LECs but they are both absorbed into the axial coupling constant g_A and the pion decay constant F_π . We only need to consider two sub-diagrams. The first one is \mathcal{M}_H . It contains $\gamma\gamma\pi NN$ vertex. Checking out the third order chiral Lagrangian [22], we list the terms which produce such vertex:

$$\mathcal{L}_{\pi N}^{(3)} = \bar{N} \left[d_8 \epsilon^{\mu\nu\alpha\beta} \langle \tilde{F}_{\mu\nu}^+ u_\alpha \rangle v_\beta + d_9 \epsilon^{\mu\nu\alpha\beta} \langle \tilde{F}_{\mu\nu}^+ \rangle u_\alpha v_\beta + d_{20} i S^\mu v^\nu [\tilde{F}_{\mu\nu}^+, v \cdot u] + d_{21} i S^\mu [\tilde{F}_{\mu\nu}^+, u^\nu] + d_{22} S^\mu [D^\nu, \tilde{F}_{\mu\nu}^-] \right] N + \dots, \quad (19)$$

where $u^2 = U = \sqrt{1 - \pi^2/F_\pi^2} + i\vec{\tau} \cdot \vec{\pi}$, $u_\mu = i(u^\dagger D_\mu u - u D_\mu u^\dagger)$ and $F_{\mu\nu}^\pm = e(\partial_\mu A_\nu - \partial_\nu A_\mu)(u Q u^\dagger \pm u^\dagger Q u)$ and $\tilde{F}_{\mu\nu}^+ = F_{\mu\nu}^+ - Tr(F_{\mu\nu}^+)$, $S_\mu = \frac{i}{2} \gamma_5 \sigma_{\mu\nu} v^\nu = (0, \frac{1}{2} \vec{\sigma})$ when v_μ is taken as $(1, \vec{0})$. The values of the LEC d_i need to be fit by the experimental data. The term with d_8 only contributes to the neutral pion photoproduction. The terms with d_8 and d_9 are both non-spinflip and will not contribute as long as the proton is unpolarized. The term with d_{20} vanishes in the Coulomb gauge. Therefore, the amplitudes with the seagull term are

$$\mathcal{A}_H^{c.t.} = \frac{e^2}{F_\pi} \left(d_{21} + \frac{d_{22}}{2} \right) [\tau_c - \delta_{c3} \tau_3] [(\vec{\epsilon}_1 \cdot \vec{\epsilon}_2^*)(\vec{\sigma} \cdot \vec{k} - \vec{q}) - (\vec{\sigma} \cdot \vec{\epsilon}_1)(\vec{\epsilon}_2^* \cdot \vec{k}) + (\vec{\sigma} \cdot \vec{\epsilon}_2^*)(\vec{\epsilon}_1 \cdot \vec{q})]. \quad (20)$$

The second sub-diagram that contains the counterterms is \mathcal{M}_D , which is the amplitude of $\pi^+ + p \rightarrow \gamma + n$, all external legs are on-shell except π^+ . The corresponding amplitude is

$$\begin{aligned} \mathcal{A}_D^{c.t.} &= \frac{-2e^2 g_A}{F_\pi} [\tau_c - \tau_3 \delta_{c3}] \left\{ \frac{\vec{\epsilon}_1 \cdot \vec{r}}{u - m_\pi^2} [d_{20} \cdot \omega_q^2 (\vec{\sigma} \cdot \vec{\epsilon}_2^*) + (d_{21} + \frac{d_{22}}{2}) [(\vec{\sigma} \cdot \vec{\epsilon}_2^*)(\omega_q^2 + \vec{q} \cdot (\vec{r} - \vec{k})) - (\vec{\sigma} \cdot \vec{q})(\vec{\epsilon}_2^* \cdot (\vec{r} - \vec{k}))]] \right\} \\ &+ \frac{\vec{\epsilon}_2^* \cdot \vec{r}}{S_1 - m_\pi^2} [d_{20} \cdot \omega_k^2 (\vec{\sigma} \cdot \vec{\epsilon}_1) + (d_{21} + \frac{d_{22}}{2}) [(\vec{\sigma} \cdot \vec{\epsilon}_1)(\omega_k^2 - \vec{k} \cdot (\vec{r} + \vec{q})) - (\vec{\sigma} \cdot \vec{k})(\vec{\epsilon}_1 \cdot (\vec{r} + \vec{q}))]] \right\} \end{aligned} \quad (21)$$

Note that the combination of $d_{21} + \frac{d_{22}}{2}$ appears in $\pi\gamma NN$ vertex as it does in $\pi\gamma\gamma NN$ vertex because the latter one is simply the minimal substitution of the former one. Both of d_{20} and $d_{21} + \frac{d_{22}}{2}$ can be fit from charge pion photoproduction and/or radiative pion capture. They also play important roles at nucleon spin polarizability γ_0 at two-loop level [24].

Now, the total cross section of the radiative photoproduction depends not only on pion polarizabilities α_{π^\pm} and β_{π^\pm} , but also on the LECs d_{20} and $d_{21} + \frac{d_{22}}{2}$,

$$\begin{aligned} \frac{d^3 \sigma_{\gamma N \rightarrow \gamma \pi N}}{dt dS_1 d\Omega} &= \left(\frac{d^3 \sigma}{dt dS_1 d\Omega} \right)^{LO} + \left(\frac{d^3 \sigma}{dt dS_1 d\Omega} \right)^{NLO} + \left(\frac{d^3 \sigma}{dt dS_1 d\Omega} \right)_0^{NNLO} \\ &+ (\tilde{\alpha} + \tilde{\beta}) \cdot \left(\frac{d^3 \sigma}{dt dS_1 d\Omega} \right)_+^{NNLO} + (\tilde{\alpha} - \tilde{\beta}) \cdot \left(\frac{d^3 \sigma}{dt dS_1 d\Omega} \right)_-^{NNLO} \\ &+ \eta \cdot \left(\frac{d^3 \sigma}{dt dS_1 d\Omega} \right)_\eta^{NNLO} + \xi \cdot \left(\frac{d^3 \sigma}{dt dS_1 d\Omega} \right)_\xi^{NNLO}. \end{aligned} \quad (22)$$

Here we define these dimensionless quantities whose sizes are $\mathcal{O}(1)$,

$$\tilde{\alpha} \pm \tilde{\beta} \equiv (\alpha_{\pi^\pm} \pm \beta_{\pi^\pm}) \cdot \frac{(4\pi F_\pi)^2 m_\pi}{\alpha_{em}}, \quad \xi \equiv \left(d_{21} + \frac{d_{22}}{2} \right) \cdot (4\pi F_\pi)^2, \quad \eta \equiv \left(d_{20} + d_{21} + \frac{d_{22}}{2} \right) \cdot (4\pi F_\pi)^2. \quad (23)$$

According to $\mathcal{O}(p^4)$ CHPT prediction (1), $\tilde{\alpha} + \tilde{\beta} = 0$ and $\tilde{\alpha} - \tilde{\beta} \simeq 1.79$. Including higher order corrections (2), $\tilde{\alpha} + \tilde{\beta} \simeq 0.12$ and $\tilde{\alpha} - \tilde{\beta} \simeq 1.49$. To extract pion polarizabilities, one should look for the kinematic conditions and

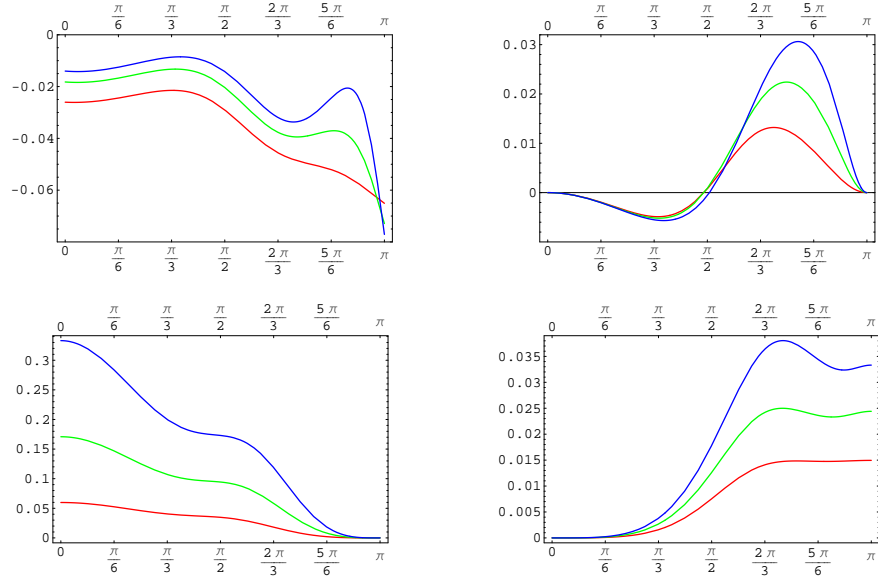


FIG. 7: R 's as functions of θ . R_ξ (left) and R_η (right) are at the upper panel. R_+ (left) and R_- (right) are at the lower panel. The red line is case of $S_1=4m_\pi^2$, the green line is case of $S_1=7m_\pi^2$. The blue line is for $S_1=10m_\pi^2$. $t=-3m_\pi^2$ for all curves.

polarization, on which both of the counterterms have the least impact of cross section. At the same time, we also have to seek the kinematic and polarization conditions which make the cross section more sensitive to the values of α_{π^\pm} and β_{π^\pm} . Therefore, we define the following dimensionless quantities R 's as

$$\begin{aligned}
 R_+ &= \left(\frac{d^3\sigma}{dt dS_1 d\Omega} \right)_+^{NNLO} / \left(\frac{d^3\sigma}{dt dS_1 d\Omega} \right)^{LO}, & R_- &= \left(\frac{d^3\sigma}{dt dS_1 d\Omega} \right)_-^{NNLO} / \left(\frac{d^3\sigma}{dt dS_1 d\Omega} \right)^{LO}, \\
 R_\eta &= \left(\frac{d^3\sigma}{dt dS_1 d\Omega} \right)_\eta^{NNLO} / \left(\frac{d^3\sigma}{dt dS_1 d\Omega} \right)^{LO}, & R_\xi &= \left(\frac{d^3\sigma}{dt dS_1 d\Omega} \right)_\xi^{NNLO} / \left(\frac{d^3\sigma}{dt dS_1 d\Omega} \right)^{LO}.
 \end{aligned} \tag{24}$$

At one hand, the kinematic and polarization conditions which gives the small values of R_ξ and R_η are preferred because it means the effects of ξ and η are small. On the other hand, we also require the kinematic conditions which give R_+ , R_- large values since it means the effects of pion polarizabilities in the total cross section is important. One important observation is that if the incoming photon is polarized along the direction perpendicular to the scattering plane, the cross section is independent of η .

We discover that R_+ is large at forward direction and R_- is large at backward direction. Moreover, both of R_+ and R_- increase when S_1 increases. Although R_+ is about 10 times larger than R_- , $\alpha_{\pi^\pm} + \beta_{\pi^\pm}$ is expected to be far smaller than $\alpha_{\pi^\pm} - \beta_{\pi^\pm}$. (According to (2) $\alpha_{\pi^\pm} - \beta_{\pi^\pm}$ is about 10 times larger than $\alpha_{\pi^\pm} + \beta_{\pi^\pm}$). Therefore, their effects are expected to be roughly of the same size. R_ξ is small and insensitive to θ at forward direction. But it becomes very sensitive to θ at backward direction, its absolute value increases dramatically in $150^\circ \leq \theta \leq 180^\circ$. R_η is very small at forward direction, increases fast during $120^\circ \leq \theta \leq 150^\circ$, then drops to zero at very backward direction. In general R_η is smaller than R_ξ . In order to measure $\alpha_{\pi^\pm} - \beta_{\pi^\pm}$, one has to measure in the range $180^\circ \geq \theta \geq 120^\circ$ and S_1 should be large because R_- is large in such a condition. However, the effects of ξ are most pronounced at very backward direction, particularly the θ dependence of R_ξ becomes very complicated at a large S_1 and very backward direction. Therefore one should avoid the region of $\theta \geq 150^\circ$. But even in the region $120^\circ \leq \theta \leq 150^\circ$, R_ξ and R_η are both comparable to R_- . We conclude that it is necessary to take the effects of ξ and η into consideration when one extract $\alpha_{\pi^\pm} - \beta_{\pi^\pm}$ from the cross section of radiative pion photoproduction. At forward direction, the effect of η is quite small but the effect of ξ is still comparable to the effect of $\alpha_{\pi^\pm} + \beta_{\pi^\pm}$. Therefore the measurement with a larger coverage of the scattering angle is requested to fit ξ , η and $\alpha_{\pi^\pm} - \beta_{\pi^\pm}$ at backward direction and fit ξ and $\alpha_{\pi^\pm} + \beta_{\pi^\pm}$ at forward direction. The polarization of the photon makes great difference. Look at the Fig(8), where the polarization vector of the incoming photon $\vec{\epsilon}_1$ is parallel to the scattering plane. R_η^\parallel is no longer smaller than R_ξ^\parallel

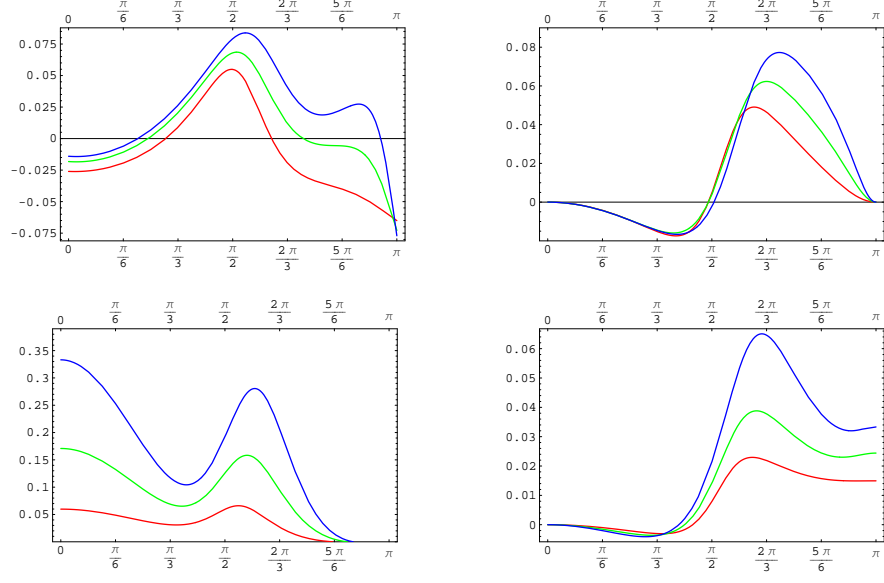


FIG. 8: R 's as functions of θ . R_ξ (left) and R_η (right) are at the upper panel. R_+ (left) and R_- (right) are at the lower panel. The red line is case of $S_1=4m_\pi^2$, the green line is case of $S_1=7m_\pi^2$. The blue line is for $S_1=10m_\pi^2$. $t=-3m_\pi^2$ for all curves.

as in the unpolarized case. One observes the bumps in R_ξ^\parallel , R_+^\parallel and R_-^\parallel between $120^\circ \geq \theta \geq 90^\circ$. Those bumps are due to the small values of $\left(\frac{d^3\sigma}{dt dS_1 d\Omega}\right)^{LO}$. Again we see that it is necessary to take the effects of ξ and η into account when one try to extract $\alpha_{\pi^\pm} - \beta_{\pi^\pm}$ ($\alpha_{\pi^\pm} + \beta_{\pi^\pm}$) at backward(forward) direction. The situation is very different when polarization vector becomes perpendicular to the scattering plane. R_η^\perp is identically zero therefore the extraction of pion polarizabilities becomes simpler. Contrasted to R_ξ^\parallel , R_ξ^\perp decreases with θ smoothly. But R_ξ^\perp is still comparable to R_-^\perp at backward direction. The extraction of $d_{21} + \frac{d_{22}}{2}$ may be interesting by itself since it plays important role in nucleon spin polarizability at $\mathcal{O}(p^5)$ [24].

One issue needed to be addressed is the contribution of the nucleon resonances, particularly the contribution of $\Delta(1232)$ resonance. It is well-known that the excitation of $\Delta(1232)$ plays important role in the spin-sector of the nucleon. It is possible to include its effect systematically in the extended version of HBChPT [23]. Here we only consider the leading order contribution of the $\Delta(1232)$ in \mathcal{M}_H . The complete analysis is out of the scope of this paper, but the leading order result in \mathcal{M}_H is very instructive. The LO diagrams with $\Delta(1232)$ are given: (see Fig(10))

$$\begin{aligned}
\mathcal{A}_\Delta^a &= \frac{-e^2 g_{\pi\Delta N} b_1}{36M_N F_\pi} [\tau_c - \tau_3 \delta_{c3}] \frac{1}{\omega_k - \Delta} \left\{ -(\vec{\epsilon}_1 \cdot \vec{\epsilon}_2^*)(\vec{\sigma} \cdot \vec{k}) + (\vec{\epsilon}_2^* \cdot \vec{k})(\vec{\sigma} \cdot \vec{\epsilon}_1) + 2i \vec{\epsilon}_2^* \cdot \vec{\epsilon}_1 \times \vec{k} \right\}, \\
\mathcal{A}_\Delta^b &= \frac{-e^2 g_{\pi\Delta N} b_1}{36M_N F_\pi} [\tau_c - \tau_3 \delta_{c3}] \frac{1}{\omega_q + \Delta} \left\{ -(\vec{\epsilon}_1 \cdot \vec{\epsilon}_2^*)(\vec{\sigma} \cdot \vec{q}) + (\vec{\epsilon}_1 \cdot \vec{q})(\vec{\sigma} \cdot \vec{\epsilon}_2^*) + 2i \vec{\epsilon}_1 \cdot \vec{\epsilon}_2^* \times \vec{q} \right\}, \\
\mathcal{A}_\Delta^c &= \frac{-e^2 g_{\pi\Delta N} b_1}{36M_N F_\pi} [\tau_c - \tau_3 \delta_{c3}] \frac{1}{\omega_k - \omega_r - \Delta} \left\{ (\vec{\epsilon}_1 \cdot \vec{\epsilon}_2^*)(\vec{\sigma} \cdot \vec{q}) - (\vec{\epsilon}_1 \cdot \vec{q})(\vec{\sigma} \cdot \vec{\epsilon}_2^*) + 2i \vec{\epsilon}_1 \cdot \vec{\epsilon}_2^* \times \vec{q} \right\}, \\
\mathcal{A}_\Delta^d &= \frac{-e^2 g_{\pi\Delta N} b_1}{36M_N F_\pi} [\tau_c - \tau_3 \delta_{c3}] \frac{1}{\omega_q + \omega_r + \Delta} \left\{ (\vec{\epsilon}_1 \cdot \vec{\epsilon}_2^*)(\vec{\sigma} \cdot \vec{k}) - (\vec{\epsilon}_2^* \cdot \vec{k})(\vec{\sigma} \cdot \vec{\epsilon}_1) + 2i \vec{\epsilon}_2^* \cdot \vec{\epsilon}_1 \times \vec{k} \right\}, \quad (25)
\end{aligned}$$

where $\Delta = M_\Delta - M_N = 293 MeV$, $g_{\pi\Delta N}$ is the coupling of $\pi N \Delta$ and b_1 is the coupling constant of $\gamma N \Delta$ [23]. Large N_c QCD gives

$$b_1 = -\frac{3}{2\sqrt{2}} \kappa_v, \quad g_{\pi\Delta N} = \frac{3}{2\sqrt{2}} g_A, \quad (26)$$

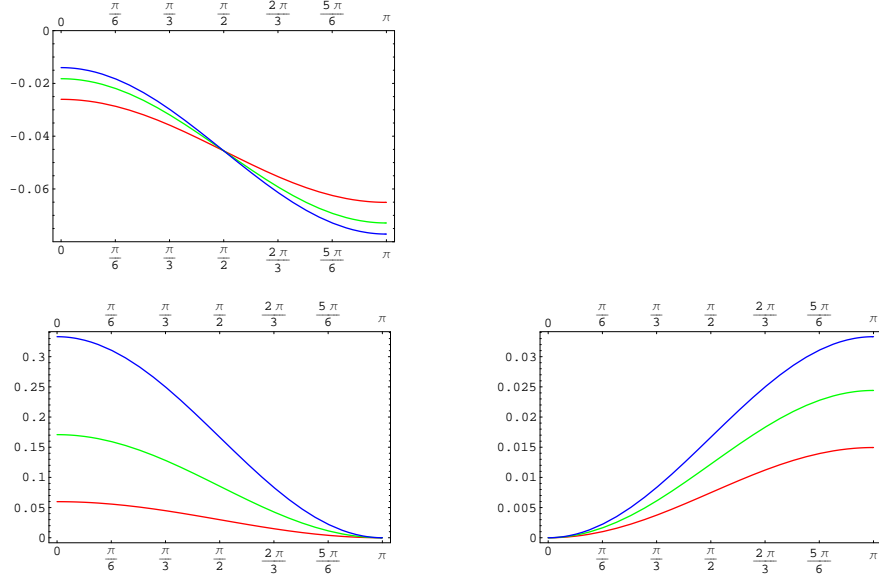


FIG. 9: R 's as functions of θ . R_ξ (left) is at the upper panel. R_+ (left) and R_- (right) are at the lower panel. The red line is case of $S_1=4m_\pi^2$, the green line is case of $S_1=7m_\pi^2$. The blue line is for $S_1=10m_\pi^2$. $t=-3m_\pi^2$ for all curves.

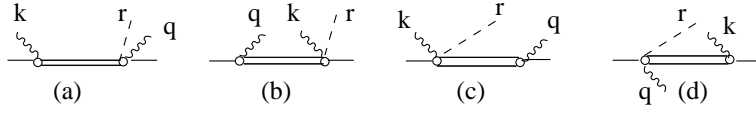


FIG. 10: The LO diagrams of radiative pion electroproduction in \mathcal{M}_H in Coulomb gauge with the intermediate $\Delta(1232)$ state.

If $\Delta \gg \omega_k, \omega_q, \omega_r$, then

$$\mathcal{A}_\Delta \simeq \frac{-e^2 g_{\pi\Delta N} b_1}{18 M_N \Delta F_\pi} [\tau_c - \delta_{c3} \tau_3] [(\vec{\epsilon}_1 \cdot \vec{\epsilon}_2^*)(\vec{\sigma} \cdot \vec{k} - \vec{q}) - (\vec{\sigma} \cdot \vec{\epsilon}_1)(\vec{\epsilon}_2^* \cdot \vec{k}) + (\vec{\sigma} \cdot \vec{\epsilon}_2^*)(\vec{\epsilon}_1 \cdot \vec{q})] \quad (27)$$

Comparing with (20), one finds that (27) has same form with (20). If one assumes that $d_{21} + \frac{d_{22}}{2}$ is saturated by $\Delta(1232)$ resonance, then one reaches the following estimate:

$$\xi \equiv (4\pi F_\pi)^2 \cdot \left(d_{21} + \frac{d_{22}}{2} \right) \simeq -\frac{1}{18} \frac{g_{\pi\Delta N} b_1}{M_N \Delta} \cdot (4\pi F_\pi)^2 \simeq 1.46. \quad (28)$$

Similarly one can find that $\eta \equiv (4\pi F_\pi)^2 \cdot (d_{20} + d_{21} + \frac{d_{22}}{2})$ is related with $N^*(1535)$. However the coupling constants of $\pi NN^*(1535)$ and $\gamma NN^*(1535)$ are unknown so one cannot make an estimate on η as (28). Also we notice that in [10] the contribution of the resonances is less important at backward direction. If the contribution of resonances is exhausted by the LEC's then our result is inconsistent with their claim. However $\Delta \simeq 2m_\pi^2$. Therefore, the complete analysis of $\Delta(1232)$ effect might be helpful to explain it.

There is another important issue need to be emphased here. Actually, the results of HBChPT on those sub-diagrams(except \mathcal{M}_H) are not unique. Because these sub-diagrams all own at least one off-shell external leg, therefore, their amplitudes depend on the parameterization of the pion fields and the nucleon field. In other words, as one can make the field transformation and the results of \mathcal{M}_A to \mathcal{M}_G will be changed. However, the physical observables are independent of the choice of parameterization of pion and nucleon fields. Therefore, if one keeps using the same parameterization to calculate different processes and use those results to extract the LEC's in the chiral Lagrangian, then there is no ambiguity at all. Note that LECs can always be extracted by some physical processes. Here we see

the advantage of the approach based on the effective field theory. For any model, even it would be very successful in describing the experimental data of sub-processes such as $\gamma + p \rightarrow \gamma + n + \pi^+$, they are not necessarily reliable to describe the whole process because of the off-shell ambiguity.

In conclusion, we suggest to extract pion polarizabilities α_{π^\pm} and β_{π^\pm} from radiative pion photoproduction $\gamma + p \rightarrow \gamma\pi^+n$ within the framework of HBCHPT. This approach is model-independent and free of any off-shell ambiguity. We find that the typical extrapolation procedure need modifications due to the diagrams such as (1-D) which has no pole at $t = m_\pi^2$ but at $u = m_\pi^2$. Our analysis showed that the main uncertainty of the extraction of the pion polarizabilities is from the effects of two combinations of the low energy constant in the chiral Lagrangian $\mathcal{L}_{\pi N}^{(3)}$, d_{20} and $d_{21} + \frac{d_{22}}{2}$. Their effects are comparable to the effects of pion polarizabilities on the cross section of radiative charged pion photoproduction. Therefore we conclude that the measurement with a larger coverage of the scattering angle is required to fit xi , η and $\alpha_{\pi^\pm} - \beta_{\pi^\pm}$ at backward direction and fit xi and $\alpha_{\pi^\pm} + \beta_{\pi^\pm}$ at forward direction. We also figure out the effect of $d_{21} + \frac{d_{22}}{2}$ is closely related to $\Delta(1232)$ resonance. The extraction of $d_{21} + \frac{d_{22}}{2}$ may be interesting by itself since it plays important role in nucleon spin polarizability at $\mathcal{O}(p^5)$ [24].

Acknowledgments

This work was supported by the US Department of Energy under Grant No. DE-FG0-97ER41048(C.-W.K) and DE-FG02-97ER41025(B.E.N and K.-B.W.). We thank Kai Schwenzer for useful suggestions and careful reading of manuscript.

APPENDIX A: AMPLITUDES OF SUB-DIAGRAM H

Here we present the amplitudes of the sub-diagrams (**H**). We use the following notations:

$$\begin{aligned} \frac{1}{i} \int \frac{d^d l}{(2\pi)^d} \frac{1}{(m_0^2 - l^2 - i\epsilon)} &= \Delta[m_0^2], \\ \frac{1}{i} \int \frac{d^d l}{(2\pi)^d} \frac{l_\mu l_\nu}{(m_0^2 - l^2)^2 - i\epsilon} &= g_{\mu\nu} M_2[m_0^2], \\ \frac{1}{i} \int \frac{d^d l}{(2\pi)^d} \frac{1}{(v \cdot l - A - i\epsilon)(m_0^2 - l^2 - i\epsilon)} &= J_0[A, m_0^2], \\ \frac{1}{i} \int \frac{d^d l}{(2\pi)^d} \frac{l_\mu}{(v \cdot l - A - i\epsilon)(m_0^2 - l^2 - i\epsilon)} &= v_\mu J_1[A, m_0^2], \\ \frac{1}{i} \int \frac{d^d l}{(2\pi)^d} \frac{l_\mu l_\nu}{(v \cdot l - A - i\epsilon)(m_0^2 - l^2 - i\epsilon)} &= g_{\mu\nu} J_2[A, m_0^2] + v_\mu v_\nu J_3[A, m_0^2]. \end{aligned}$$

Using the dimensional regularization one obtained

$$\begin{aligned} \Delta_0[m_0^2] &= 2m_0^2 \left(L + \frac{1}{16\pi^2} \ln \frac{m_0}{\mu} \right), \\ M_2[m_0^2] &= \frac{1}{d} \left[\Delta_0[m_0^2] + m_0^2 \cdot \frac{d\Delta_0[m_0^2]}{dm_0^2} \right], \\ J_0[A, m_0^2] &= -4AL + \frac{A}{8\pi^2} \left(1 - 2 \ln \frac{m_0}{\mu} \right) - \frac{1}{4\pi^2} \sqrt{m_0^2 - A^2} \cdot \cos^{-1} \left(\frac{-A}{m_0} \right), \\ J_1[A, m_0^2] &= A \cdot J_0[A, m_0^2] + \Delta_0[m_0^2], \\ J_2[A, m_0^2] &= \frac{1}{d-4} [(m_0^2 - A^2) J_0[A, m_0^2] - A \cdot \Delta_0[m_0^2]], \\ J_3[A, m_0^2] &= A \cdot J_1[A, m_0^2] - J_2[A, m_0^2], \\ L &= \frac{\mu^{d-4}}{16\pi^2} \left[\frac{1}{d-4} + \frac{1}{2} (\gamma_E - 1 - \ln 4\pi) \right], \end{aligned}$$

here μ is the renormalization scale and $\gamma_E = 0.577215\dots$ is the Euler number. d is the space-time dimensions. Also we define $w = (k - q)^2$ and $J_0^{(m)} \equiv \frac{\partial^m J_0[A, m_0^2]}{\partial (m_0^2)^m}$. The results are

$$\begin{aligned}
\mathcal{M}_{H1} &= \frac{-\sqrt{2}e^2 g_A^2}{2F_\pi^3} \int_0^1 dy \int_0^{1-y} dx \\
&(\vec{\epsilon}_1 \cdot \vec{\epsilon}_2^*)(\vec{\sigma} \cdot \vec{k})(x+y) \left[M_2^{(1)}[m_\pi^2 + y(y-1)w + xyw] + 2\omega_r J_2^{(2)}[x\omega_k + y\omega_r, m_\pi^2 + y(y-1)w + xyw] \right] \\
&+ (\vec{\epsilon}_1 \cdot \vec{\epsilon}_2^*)(\vec{\sigma} \cdot \vec{q})(-y) \left[M_2^{(1)}[m_\pi^2 + y(y-1)w + xyw] + 2\omega_r J_2^{(2)}[x\omega_k + y\omega_r, m_\pi^2 + y(y-1)w + xyw] \right] \\
&+ (\vec{\sigma} \cdot \vec{\epsilon}_1)(\vec{\epsilon}_2^* \cdot \vec{k})(x+y - \frac{1}{2}) \left[M_2^{(1)}[m_\pi^2 + y(y-1)w + xyw] + 2\omega_r J_2^{(2)}[x\omega_k + y\omega_r, m_\pi^2 + y(y-1)w + xyw] \right] \\
&+ (\vec{\sigma} \cdot \vec{\epsilon}_2^*)(\vec{\epsilon}_1 \cdot \vec{q})(x+y-1) \left[M_2^{(1)}[m_\pi^2 + y(y-1)w + xyw] + 2\omega_r J_2^{(2)}[x\omega_k + y\omega_r, m_\pi^2 + y(y-1)w + xyw] \right] \\
&+ (\vec{\epsilon}_1 \cdot \vec{q})(\vec{\epsilon}_2^* \cdot \vec{k})(\vec{\sigma} \cdot \vec{k})[y(x+y)(x+y-1)] \left[\Delta_0^{(2)}[m_\pi^2 + y(y-1)w + xyw] + 2\omega_r J_0^{(2)}[x\omega_k + y\omega_r, m_\pi^2 + y(y-1)w + xyw] \right] \\
&- (\vec{\epsilon}_1 \cdot \vec{q})(\vec{\epsilon}_2^* \cdot \vec{k})(\vec{\sigma} \cdot \vec{q})y^2(x+y-1) \left[\Delta_0^{(2)}[m_\pi^2 + y(y-1)w + xyw] + 2\omega_r J_0^{(2)}[x\omega_k + y\omega_r, m_\pi^2 + y(y-1)w + xyw] \right]
\end{aligned} \tag{A1}$$

$$\begin{aligned}
\mathcal{M}_{H2} &= \frac{-\sqrt{2}e^2 g_A^2}{2F_\pi^3} \int_0^1 dy \int_0^{1-y} dx \\
&(\vec{\epsilon}_1 \cdot \vec{\epsilon}_2^*)(\vec{\sigma} \cdot \vec{q})(x+y) \left[M_2^{(1)}[m_\pi^2 + y(y-1)w + xyw] - 2\omega_r J_2^{(2)}[x\omega_q - y\omega_r, m_\pi^2 + y(y-1)w + xyw] \right] \\
&+ (\vec{\epsilon}_1 \cdot \vec{\epsilon}_2^*)(\vec{\sigma} \cdot \vec{k})(-y) \left[M_2^{(1)}[m_\pi^2 + y(y-1)w + xyw] - 2\omega_r J_2^{(2)}[x\omega_q - y\omega_r, m_\pi^2 + y(y-1)w + xyw] \right] \\
&+ (\vec{\sigma} \cdot \vec{\epsilon}_2^*)(\vec{\epsilon}_1 \cdot \vec{q})(x+y - \frac{1}{2}) \left[M_2^{(1)}[m_\pi^2 + y(y-1)w + xyw] - 2\omega_r J_2^{(2)}[x\omega_q - y\omega_r, m_\pi^2 + y(y-1)w + xyw] \right] \\
&+ (\vec{\sigma} \cdot \vec{\epsilon}_1)(\vec{\epsilon}_2^* \cdot \vec{k})(x+y-1) \left[M_2^{(1)}[m_\pi^2 + y(y-1)w + xyw] - 2\omega_r J_2^{(2)}[x\omega_q - y\omega_r, m_\pi^2 + y(y-1)w + xyw] \right] \\
&+ (\vec{\epsilon}_2^* \cdot \vec{k})(\vec{\epsilon}_1 \cdot \vec{q})(\vec{\sigma} \cdot \vec{q})[y(x+y)(x+y-1)] \left[\Delta_0^{(2)}[m_\pi^2 + y(y-1)w + xyw] - 2\omega_r J_0^{(2)}[x\omega_q - y\omega_r, m_\pi^2 + y(y-1)w + xyw] \right] \\
&- (\vec{\epsilon}_2^* \cdot \vec{k})(\vec{\epsilon}_1 \cdot \vec{q})(\vec{\sigma} \cdot \vec{k})y^2(x+y-1) \left[\Delta_0^{(2)}[m_\pi^2 + y(y-1)w + xyw] - 2\omega_r J_0^{(2)}[x\omega_q - y\omega_r, m_\pi^2 + y(y-1)w + xyw] \right]
\end{aligned} \tag{A2}$$

$$\mathcal{M}_{H3} = \frac{\sqrt{2}e^2 g_A^2}{4F_\pi^3} (\vec{\sigma} \cdot \vec{k} - \vec{q})(\vec{\epsilon}_1 \cdot \vec{\epsilon}_2^*) \int_0^1 dx x \cdot \{ \Delta_0^{(1)}[m_\pi^2 + x(x-1)w] + 2\omega_r J_0^{(1)}[x\omega_r, m_\pi^2 + x(x-1)w] \}. \tag{A3}$$

$$\mathcal{M}_{H4} = -\frac{\sqrt{2}e^2 g_A^2}{4F_\pi^3} (\vec{\sigma} \cdot \vec{k} - \vec{q})(\vec{\epsilon}_1 \cdot \vec{\epsilon}_2^*) \int_0^1 dx (1-x) \cdot \{ \Delta_0^{(1)}[m_\pi^2 + x(x-1)w] + 2\omega_r J_0^{(1)}[(x-1)\omega_r, m_\pi^2 + x(x-1)w] \}. \tag{A4}$$

$$\mathcal{M}_{H5} = \mathcal{M}_{H6} = 0. \tag{A5}$$

$$\begin{aligned}
\mathcal{M}_{H7} &= -\frac{\sqrt{2}e^2 g_A^2}{F_\pi^3} (\vec{\sigma} \cdot 3\vec{k} - 3\vec{q} - 2\vec{r}) \{ (\vec{\epsilon}_1 \cdot \vec{\epsilon}_2^*) \int_0^1 dy \int_0^{1-x} dy (-1) \cdot M_2^{(1)}[m_\pi^2 + y(y-1)w + xyw] \\
&+ (\vec{\epsilon}_1 \cdot \vec{q})(\vec{\epsilon}_2^* \cdot \vec{k}) \int_0^1 dy \int_0^{1-x} dy y(1-x-y) \Delta_0^{(2)}[m_\pi^2 + y(y-1)w + xyw] \}.
\end{aligned} \tag{A6}$$

$$\mathcal{M}_{H8} = \frac{\sqrt{2}e^2 g_A^2}{2F_\pi^3} (\vec{\sigma} \cdot 3\vec{k} - 3\vec{q} - 2\vec{r})(\vec{\epsilon}_1 \cdot \vec{\epsilon}_2^*) \int_0^1 dx (-1) \cdot \{ \Delta_0^{(1)}[m_\pi^2 + x(x-1)w] \}. \tag{A7}$$

$$\mathcal{M}_{H9} = \frac{\sqrt{2}e^2}{F_\pi} \left(d_{21} + \frac{d_{22}}{2} \right) [(\vec{\epsilon}_1 \cdot \vec{\epsilon}_2^*)(\vec{\sigma} \cdot \vec{k} - \vec{q}) - (\vec{\sigma} \cdot \vec{\epsilon}_1)(\vec{\epsilon}_2^* \cdot \vec{k}) + (\vec{\sigma} \cdot \vec{\epsilon}_2^*)(\vec{\epsilon}_1 \cdot \vec{q})] \quad (\text{A8})$$

Here we does not explicitly display the results of cross diagrams which can be get by exchanging $\vec{k} \longleftrightarrow -\vec{q}$, $\vec{\epsilon}_1 \longleftrightarrow \vec{\epsilon}_2^*$.

-
- [1] J. Bijenens and F. Cornet, Nucl. Phys. **B 296**, 557 (1988), J. F. Donoghue, B. R. Holstein, Phys. Rev **D 40**, 2378 (1989), B. R. Holstein, Comm. Nucl. Part. Phys. **19**, 221 (1990).
 - [2] J. Gasser and H. Leutwyler, Annals Phys.**158**, 142 (1984).
 - [3] E. Frlež et al. hep-ex/0312029.
 - [4] S. Bellucci, J. Gasser and M.E. Sainio, Nucl. Phys. **B 423** 80 (1994).
 - [5] U. Bürgi, Nucl. Phys. **479**, 392(1997).
 - [6] Yu. M. Antipov et al, Phys. Lett. **B 121**, 445 (1983), Z. Phys. **C 26**, 495 (1988).
 - [7] T. Aibergenov et al. Proc. of the Lebedev Phys. Inst. **186**, 169 (1988).
 - [8] J. Boyer et al, Phys. Rev. **D 42**, 1350 (1990).
 - [9] D. Babusci, S. Bellucci, G. Giordano, G. Matone, A. M. Sandorfi , M. A. Moinester, Phys. Lett. **B 277**, 158 (1992).
 - [10] J. Ahrens, nucl-ex/0407011.
 - [11] V. Bernard, N. Kaiser and Ulf-G. Meissner, Int. J. Mod. Phys **E4**, 193 (1995).
 - [12] L. Fil'kov , Sov.J.Nucl.Phys. **41** 636(1985).
 - [13] D. Drechsel and L. Fil'kov, Z. Phys. **A349**, 177(1994).
 - [14] G. Chew et al., Phys. ReV **106**, 1345 (1957).
 - [15] C.-W.Kao, B.E.Norum and K.-B. Wang, in preparation.
 - [16] C. Unkmeir, A. Ocherachvili, T. Fuchs, M.A. Moinester,S. Scherer Phys. Rev **C 65**, 015206(2002).
 - [17] C. Unkmeir, S. Scherer, A. IL'vov and D. Drechsel , Phys. Rev. **D61**, 034002(2000).
 - [18] H.W. Fearing, T.R. Hemmert, R. Lewis and C. Unkmeir, Nucl. Phys. **A 684**, 377(2001), Phys. Rev. **C62**, 054006(2000).
 - [19] V. Bernard, N. Kaiser, J. Kambor and Ulf-G. Meissner Nucl. Phys. **B388**, 315(1992).
 - [20] J. Wess and B. Zumino, Phys. Lett. **B37**, 95 (1971), E. Witten, Nucl. Phys. **B 223**, 422 (1983).
 - [21] J. S. Bell and R. Jackiw, Nuovo Cimento **60A**, 47 (1969), S. Adler, Phys. Rev. **177**, 2426, (1969).
 - [22] N. Fettes,U. Meissner, and S. Steininger , Nucl. Phys. **A640**, 199(1998).
 - [23] T. R. Hemmert, B. R. Holstein and J. Kambor, J. Phys. G **24**, 1831 (1998).
 - [24] C.-W. Kao and J. A. McGovern, will appears in the proceedings of the third International Symposium on the Gerasimov-Drell-Hearn sum rule and the spin structure of the nucleon, Norfolk, Virginia, June 2-5, 2004.